

# Universal dynamics of density correlations at the transition to many-body localized state

M. Mierzejewski,<sup>1</sup> J. Herbrych,<sup>2</sup> and P. Prelovšek<sup>3,4</sup>

<sup>1</sup>*Institute of Physics, University of Silesia, 40-007 Katowice, Poland*

<sup>2</sup>*Crete Center for Quantum Complexity and Nanotechnology, Department of Physics, University of Crete, P.O. Box 2208, 71003 Heraklion, Greece*

<sup>3</sup>*Jožef Stefan Institute, SI-1000 Ljubljana, Slovenia*

<sup>4</sup>*Faculty of Mathematics and Physics, University of Ljubljana, SI-1000 Ljubljana, Slovenia*

Within one-dimensional disordered models of interacting fermions we perform a numerical study of several dynamical density correlations, which can serve as hallmarks of the transition to the many-body localized state. Results confirm that density-wave correlations exhibit quite abrupt change with the increasing disorder, with nonvanishing long-time value characteristic for nonergodic phase. In addition, our results reveal in a wide time-window a logarithmic variation of correlations in time, which we can bring in connection with the anomalous behavior of the dynamical conductivity near the transition. Our result support the view that transition to many-body localization can be characterized by universal dynamical exponents.

PACS numbers: 71.23.-k, 71.27.+a, 71.30.+h, 71.10.Fd

## I. INTRODUCTION

The idea of many-body localization (MBL) emerged from the well understood Anderson localization of non-interacting (NI) fermions,<sup>1–4</sup> by taking into account the many-body interaction.<sup>5,6</sup> The basic claim that localization can, at large disorder, persist in the whole spectrum and consequently at all temperatures, has been by now supported by numerous studies on one-dimensional (1D) disordered models. There are essential features of the MBL phase<sup>7–17</sup> which have been confirmed numerically, predominantly for interacting spinless fermions: the change of the level statistics from a Wigner-Dyson to a Poisson-like in the nonergodic phase,<sup>18</sup> the vanishing of d.c. transport at any  $T$ <sup>19–25</sup> even beyond the regime of the linear response<sup>26</sup>, the logarithmic growth of the entanglement entropy in the MBL phase,<sup>27–33</sup> the nonergodic behavior of correlation functions related also with the existence of local conserved quantities.<sup>30,31,34–49</sup>

Experimental support for the MBL comes so far from studies of cold-atom systems.<sup>37,50–52</sup> Absence of d.c. transport under constant force<sup>50</sup> and the nonergodic evolution of initially quenched state<sup>37,51</sup> have been used as the experimental criteria. In particular, in the latter studies the long-time remainder of the charge imbalance has been used as a practical hallmark of the MBL which becomes finite within the nonergodic phase. Such a quantity is a natural counterpart of the d.c. transport quantities, as e.g., the d.c. conductivity  $\sigma_0$  being nonzero in the “normal” ergodic phase (including also the possibility of subdiffusive transport).<sup>19–23</sup> However, the detailed theoretical and numerical analysis of such indicators of the MBL is still missing.<sup>31,37</sup> On the other hand, several numerical calculations of dynamical conductivity<sup>21,24,25</sup> as well as more general studies of dynamics using the renormalization-group approach<sup>22,31,53,54</sup> indicate that the transition is primarily characterized by dynamical critical exponent, e.g. of the dynamical conductivity  $\sigma(\omega)$ .

In this paper, we study dynamical density correlations within the prototype 1D model of the MBL system. We concentrate on the aspect how the Anderson localization, established for NI fermions in 1D for any disorder strength  $W$ , is

destroyed by a modest repulsive interaction  $V$ . In particular, we study the time-dependent density-wave (DW) correlation functions  $C(t)$ , closely related to the charge imbalance.<sup>31,37,51</sup> We show that  $C(t = \infty)$  reveal quite sharp transition at large disorder  $W \sim W_c$ , hence they can serve as hallmarks of the MBL phase. In addition, our results show so far novel and universal logarithmic time-dependence of  $C(t)$  in a very wide time-range being particularly extended near the MBL transition. Using the memory-function analysis we show that this anomalous density dynamics is closely related to the scaling of the dynamical conductivity, confirming that such universal dynamical scaling appears to be more fundamental hallmark of the MBL than the stationary value  $C(t = \infty)$  itself. Finally, we find evidence that such anomalous dynamics is characteristic also for other disordered systems with no apparent connection with NI Anderson localization.

## II. MODEL AND NUMERICAL METHODS.

We consider the prototype model for the MBL, i.e. the 1D model of interacting spinless fermions with random local potentials,

$$H = -t_0 \sum_i \left( c_{i+1}^\dagger c_i + \text{H.c.} \right) + \sum_i h_i \tilde{n}_i + H_V, \quad (1)$$

$$H_V = V \sum_i \tilde{n}_{i+1} \tilde{n}_i, \quad (2)$$

where  $\tilde{n}_i = n_i - 1/2 = c_i^\dagger c_i - 1/2$ . We take quenched disorder  $h_i$  with a uniform distribution  $-W < h_i < W$ . The model (1) is in 1D equivalent to the anisotropic Heisenberg model with random fields. Taking in the following  $t_0 = 1$  as the energy unit, we mostly consider cases of modest interaction  $V/t_0 = 1$  being closer to the NI case  $V = 0$ . We also fix the density of fermions to half-filling, i.e. having  $N = L/2$  fermions on a system with  $L$  sites and with periodic boundary conditions. Since the MBL at larger  $W$  occurs at any temperature, we study the limiting case  $T \rightarrow \infty$  being

the optimal one for numerical calculations. However, in the Appendix A we show also results for finite temperatures.

The dynamical quantities are obtained mainly from exact diagonalization (ED) of the Hamiltonian, (1), where one can reach  $L = 16$ . Further on we also perform calculations of the DW correlations using the microcanonical Lanczos method (MCLM),<sup>55,56</sup> very suitable for the study of dynamical quantities at  $T \gg 1$  and allowing for substantially larger system, e.g.,  $L = 24$ . In the latter method, the main restriction is finite frequency resolution of dynamical spectra, with typically  $\delta\omega \sim 10^{-3}$  (for  $\sim 10^4$  Lanczos steps) restricting the reachable times  $t < 1000$ .

### III. DENSITY-WAVE CORRELATIONS.

As a very practical tool to investigate nonergodicity in disordered system, we employ the staggered DW operator  $O_s$ , and its normalized autocorrelation function

$$O_s = \sum_i (-1)^i n_i, \quad (3)$$

$$C_s(t) = \left\langle \frac{\text{Tr}(O_s e^{iHt} O_s e^{-iHt})}{\text{Tr}(O_s^2)} \right\rangle. \quad (4)$$

$C_s(t)$  can be directly related to the time-dependent imbalance measured in the cold-atom systems.<sup>37,51</sup> Since  $C_s(t \rightarrow \infty) > 0$  marks a nonergodic behavior, the stiffness  $C_s(\infty)$  can be used as an indicator for the MBL transition. Here,  $\langle \dots \rangle$  represents average over  $\sim 10^2 \div 10^3$  configurations of  $h_i$ .

The decay of  $C_s(t)$  is at short  $t \sim 1$  masked by oscillations with frequency  $\omega = 2$  which emerge from  $H_0$  only.<sup>26,31,37</sup> These oscillations are clearly visible in Fig. 1. As discussed later on, they can also be observed from the Fourier transform  $C_s(\omega) = 1/2\pi \int_{-\infty}^{\infty} dt \exp(i\omega t) C_s(t)$ . It is convenient to consider also a modified DW operator

$$O_l = \sum_l (-1)^l \varphi_l^\dagger \varphi_l, \quad (5)$$

as well as the corresponding correlation function  $C_l(t)$ . Index  $l$  enumerates sorted energies of the single-particle Hamiltonian,  $H - H_V = \sum_l \epsilon_l \varphi_l^\dagger \varphi_l$ . Consequently, labelling the position of the localized states by  $l$  is to some extent arbitrary. The correlation function  $C_s(t)$  describes the decay of the initial staggered density wave with the wave-vector  $q = \pi$ . Contrary to this,  $C_l(t)$  describes how/whether the system retains the information about a random density distribution. Here, we search for common properties of both correlation functions which should be generic for most of the spatial particles distributions. Note also that the decay of  $C_l(t)$  is solely due to many-body interactions, while  $C_l(t) = 1$  for  $V = 0$ .

In order to further demonstrate universality of the long-time behavior we study also a system with a homogeneous single-particle Hamiltonian ( $h_i = 0$ ) but with a disordered many-body interaction<sup>57</sup>

$$H_V \rightarrow \tilde{H}_V = \sum_i 2V_i \tilde{n}_{i+1} \tilde{n}_i + V' \sum_i \tilde{n}_{i+2} \tilde{n}_i, \quad (6)$$

where  $V_i \geq 0$  (positive to avoid localization due to bound states) are uniformly distributed variables,  $0 \leq V_i \leq 2W$ . We study the autocorrelation function  $C_V(t)$  for the related DW operator

$$O_V = \sum_i (-1)^i \tilde{n}_{i+1} \tilde{n}_i. \quad (7)$$

The DW decay function  $C_s(t)$  is calculated numerically using both methods described above.  $C_l(t)$  and  $C_V(t)$  are obtained from ED. In the Appendix B we show for moderate time-window that  $C_l(t)$  can also be obtained in a reduced basis for larger systems than accessible for ED calculations.  $C_s(t)$  and  $C_l(t)$  are obtained for the Hamiltonian (1) with  $V = 1$ , while  $C_V(t)$  for interaction (6) with  $V' = 1$ . Whenever our discussion applies to all correlation functions, we omit subscripts  $s, l, V$  denoting  $C = C_{(s,l,V)}$  and  $O = O_{(s,l,V)}$ . To recognize the essential features corresponding to  $t \gg 1$  (or  $\omega \ll 1$ ) it is convenient to present the integrated spectra

$$I(\tau) = \int_{-1/\tau}^{1/\tau} d\omega C(\omega) = \left\langle \frac{\mathcal{I}(\tau)}{\mathcal{I}(\tau \rightarrow 0^+)} \right\rangle, \quad (8)$$

$$\mathcal{I}(\tau) = \sum_{\alpha, \alpha'} \theta \left( \frac{1}{\tau} - |E_\alpha - E_{\alpha'}| \right) |\langle \alpha | O | \alpha' \rangle|^2, \quad (9)$$

where  $H|\alpha\rangle = E_\alpha|\alpha\rangle$ . When carrying out the ED calculations we first obtain  $\mathcal{I}(\tau)$  from Eq. (9) and then  $C(\omega)$  by differentiating Eq. (8). Neglecting accidental degeneracies,  $C(t \rightarrow \infty)$  can formally be obtained from Eqs. (8) and (9) by restricting summation to diagonal terms  $\alpha = \alpha'$ . In Figure 1 we compare the real-time correlation function  $C_s(t)$  with the integrated spectrum  $I_s(\tau)$ . Note that  $I(\tau)$  represent to some extent the real- $t$  evolution, since  $I(t) = C(t)$  in both limits  $t \rightarrow 0$  and  $t \rightarrow \infty$ . Since  $I(\tau)$  doesn't show the transient oscillations, it is more convenient to use the latter quantity for the studies of the long-time dynamics which turns out to be very slow.

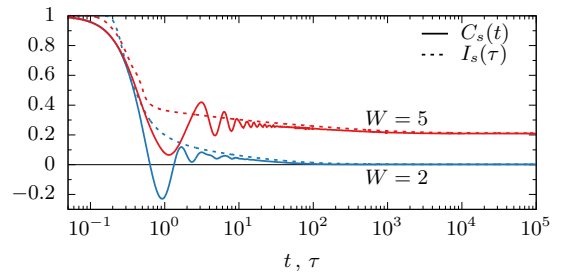


Figure 1. (Color online) Comparison of the real-time correlation function  $C_s(t)$  and the integrated spectrum  $I_s(\tau)$  obtained from ED for  $L = 16$  with weak ( $W = 2$ ) and strong ( $W = 5$ ) disorder.

Results for  $I(\tau)$  in Figs. 2 and 3 allow for several conclusions: (a) Qualitative behavior of all  $I(\tau)$  is quite similar. (b) ED results at fixed  $L$  always reveal finite  $C(\infty) = I(\infty) > 0$ . These results are plotted in Fig. 3 vs.  $1/L$  and show that for

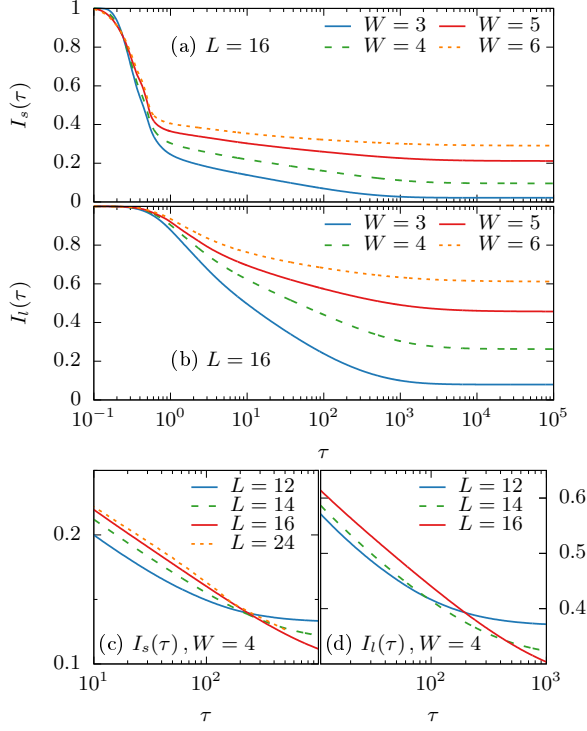


Figure 2. (Color online) Integrated correlation functions  $I_{s,l}(\tau)$ , obtained from ED ( $L \leq 16$ ) and MCLM ( $L = 24$ ) for different disorder strengths  $W$ .

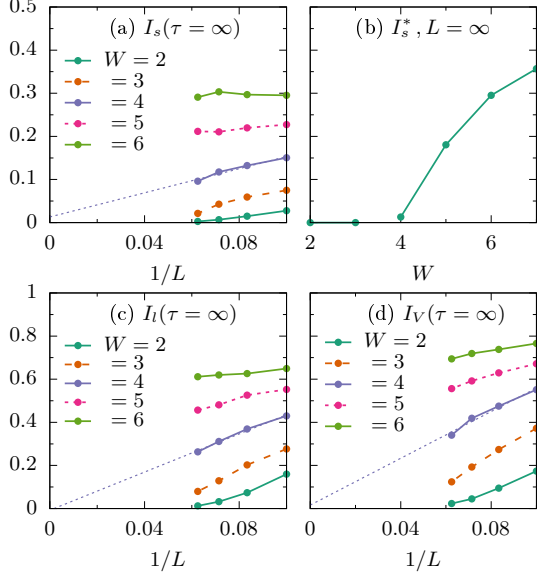


Figure 3. (Color online)  $1/L$  scaling of stiffnesses  $I_{s,l,V}(\infty)$ , obtained from ED. Note that  $C(t \rightarrow \infty) = I(\infty)$ . (b) shows the extrapolated value  $I_s^*$ .

$W < W_c \sim 4$  the scaled values vanish, in agreement with previous studies<sup>23</sup> of the model (1). It is interesting that roughly the same  $W_c$  is obtained for a system with the disordered interaction (6). For  $W > W_c$ , the extrapolation  $L \rightarrow \infty$  leads to

finite stiffnesses  $I^*$ , which can be used as convenient indicator for the MBL phase.<sup>37</sup> (c) Most remarkable, all  $I(\tau)$  reveal for  $W \geq 3$  a very wide time-window beyond  $\tau > 1$  with a slow, logarithmic-like decay, e.g.  $I(\tau) \sim a - b \log(\tau)$ . As shown in Figs. 2c and 2d, this behavior is particularly clear at the transition  $W \simeq W_c$ . In the latter case, deviations from the logarithmic time-dependence diminish when the system size increases, hence these deviations seem to represent the finite-size effects. Such a decay extends typically to  $\tau^* \sim 1000$  for largest systems  $L = 16$  available for ED, before saturating at  $C(\infty)$ . The decay continues apparently to the largest  $\tau^* \sim 1000$  available by MCLM ( $L = 24$ ). The comparison of results for different  $L$  confirms that  $\tau^*$  can extend at least for one decade when increasing the system from  $L = 12$  to  $L = 16$ .

While the observations (a) and (b) have been at least partly reported before, the universality of the slow (logarithmic) variation<sup>58,59</sup> appears to be a novel one. It is evident that  $I(\tau) \propto \log(\tau)$  has to emerge from an anomalous  $\omega$ -dependence. Taking the ED results at finite  $L$  as the input, it requires

$$C(\omega) = A\delta(\omega) + C^{\text{reg}}(\omega), \quad (10)$$

$$C^{\text{reg}}(\omega \ll 1) = B/[\omega^\zeta + \Delta^\zeta]. \quad (11)$$

Here,  $A = C(t \rightarrow \infty)$  is the stiffness, while  $C^{\text{reg}}(\omega)$  represents the regular part. We note that at finite  $L$  the latter is meaningful only for  $\omega > \delta_0$  where  $\delta_0$  is typical level spacing (with  $\delta_0 \sim 10^{-2}, 10^{-3}$  for  $L = 12, 16$ , respectively). We display in Fig. 4 the ED results for  $C^{\text{reg}}(\omega)$  on a log scale, which clearly reveal that  $\zeta \leq 1$  in a wide range of  $W$  in the vicinity of  $W \sim W_c$ . On the other hand, the saturation with  $\Delta \sim 10^{-2} > \delta_0$  is among results well resolved only in the case of weak disorder, i.e.  $W = 2$ . The question remains whether  $\Delta$  is finite also, e.g. for  $W=3$ . Still, our results in Fig. 4c strongly suggest that  $\Delta$  vanishes within the MBL phase, i.e. for  $W > W_c$ , while more detailed behavior of  $\Delta$  in the regime  $W \lesssim W_c$  remains an open problem. A strict logarithmic dependence of  $C(t)$  implies that  $\zeta \rightarrow 1$ , whereas Fig. 4 shows that  $\zeta$  is close to but smaller than 1 leading to time dependence as  $t^{-\varepsilon}$ , with  $\varepsilon = 1 - \zeta > 0$ . We cannot judge whether this tiny deviations are real or show up as numerical artifacts. However, since  $t^{-\varepsilon} = 1 - \varepsilon \log(t) + O[\varepsilon^2 \log(t)^2]$  such deviations may become relevant first for long times  $t \sim \exp(1/\varepsilon)$ .

#### IV. THE RELATION TO DYNAMICAL CONDUCTIVITY

In order to relate such a behavior to other dynamical observables, it is convenient to analyze the full complex response function

$$\tilde{C}(\omega) = (i/\pi) \int_0^\infty dt \exp(i\omega t) C(t), \quad (12)$$

so that  $\tilde{C}''(\omega) = C(\omega)$ . Since  $\tilde{C}(\omega)$  is analytical function of  $\omega$  (for  $\Im\omega > 0$ ), it can be represented in terms of the complex

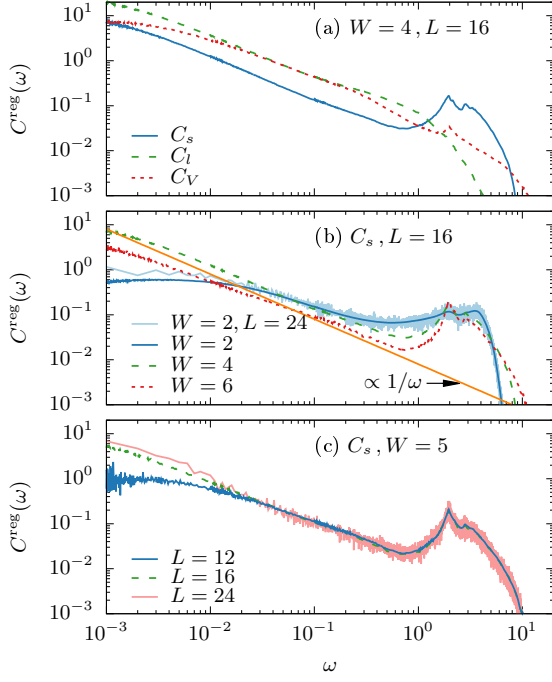


Figure 4. (Color online) Regular parts of DW correlation spectra  $C^{\text{reg}}(\omega)$ , obtained via ED ( $L \leq 16$ ) and MCLM ( $L = 24$ ). In (b) we include for reference the marginal behavior  $C^{\text{reg}}(\omega) \propto 1/\omega$ . Note that contrary to other correlation functions,  $C_s(\omega)$  has a strong peak at  $\omega = 2$ .

memory function  $M(\omega)$ . Taking into account the normalization  $C(t=0) = 1$  one gets

$$\tilde{C}(\omega) = -(1/\pi)[\omega + M(\omega)]^{-1}. \quad (13)$$

In particular, for the DW correlations  $C_s(\omega)$ ,  $M(\omega)$  is related to (an effective) dynamical conductivity at the same  $q = \pi$ , i.e.,  $M''(\omega) \sim \sin^2(q/2)\tilde{\sigma}'(q, \omega)$ . Note, however, that  $\tilde{\sigma}(q, \omega)$  is the current response function only in the limit  $q \rightarrow 0$ .<sup>60–62</sup> In general, the representation of  $C(\omega)$ , Eq. (13), in terms of  $M(\omega)$  has a clear advantage that instead of diverging  $C(\omega \rightarrow 0)$ , we are dealing with a regular  $\Gamma(\omega) = M''(\omega) > 0$ , representing the DW relaxation-rate function. Results obtained for all correlation functions are compared in Fig. 5.

Our results indicate on two regimes with qualitatively different dynamics. For  $W < W_c \sim 4$ , our results are consistent with vanishing stiffness in the thermodynamic limit, i.e.,  $A = 0$  and only  $C^{\text{reg}}$  remains in Eq. (10). Then,  $\Delta$  is non-vanishing at least for weaker disorder  $W \leq 2$ . Consequently, also  $\Gamma(\omega \rightarrow 0) > 0$  still being much smaller than corresponding maxima appearing at  $\omega \sim 1$ . Such  $\Gamma(\omega)$  has very close similarity to  $q \rightarrow 0$  optical conductivity,  $\sigma(\omega)$ ,<sup>20,24,25</sup> with the form  $\Gamma(\omega \ll 1) \sim \Gamma_0 + g\omega^\alpha$ , where  $\alpha = \zeta \leq 1$  and  $\Gamma_0 \propto \Delta^\zeta$ .

For  $W > W_c$  the nonergodic contribution  $A > 0$  is unavoidable. The latter leads to  $\Gamma(\omega) \sim \omega^\alpha$  with  $\alpha = 2 - \zeta$ . It is evident that the marginal case corresponds to  $\zeta = 1$  and  $\alpha = 1$ , which is another criterion for the MBL transition. Our

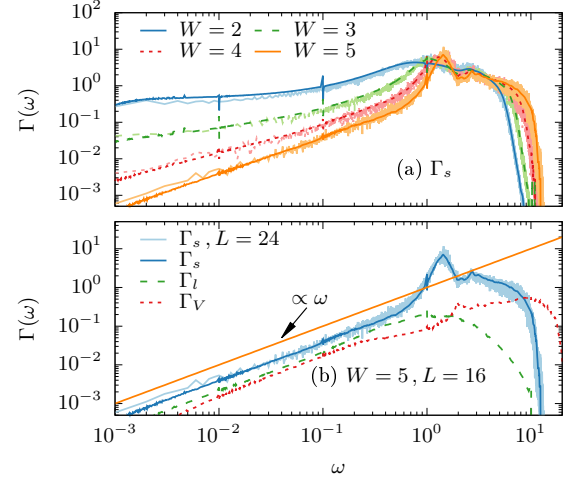


Figure 5. (Color online) DW relaxation-rate functions  $\Gamma(\omega)$ , as calculated via the ED and MCLM for  $L = 16$  and  $L = 24$  (nearly overlapping curves), respectively. In (a)  $\Gamma_s(\omega)$  is shown for various  $W$  with  $L = 16$  and  $L = 24$ , while (b) displays various  $\Gamma(\omega)$  for fixed  $W \geq W_c$ .

results (not shown) indicate that for  $W \gg W_c$  the critical exponent is increasing,  $\alpha > 1$ , nevertheless we find in a broad range of  $W$  nearly constant  $\alpha \sim 1$ .

## V. CONCLUSIONS

We presented numerical results for several dynamical density correlations. We have shown that the correlation functions display universal long-time behavior. It holds true for the prototype MBL Hamiltonian as well as for a system with homogenous single-particle Hamiltonian but with disordered many-body interaction.<sup>57</sup> All quantities reveal a nonergodic behavior, well visible in the stiffnesses,  $C(t \rightarrow \infty) > 0$ , which remain finite even after the extrapolation of finite-size results to  $L \rightarrow \infty$ . In this sense, the extrapolated values  $C^*$  can be used as indicators of the nonergodic MBL phase, in direct correspondence to the imbalance stiffness in the cold-atom experiments.<sup>31,37</sup>

Still, the main message of our study is that all the correlation functions  $C(t)$  exhibit near the MBL transition anomalously slow relaxation towards the presumable  $t \rightarrow \infty$  limit. Such a logarithmic time-dependence is visible over several decades in the window  $1 < t < t^*$  where  $t^* > 1000$  seems to be limited at  $W \geq W_c$  only by finite size restrictions of our numerical methods. Although we are dealing in our study with DW at wave-vectors  $q \gg 0$ , our analysis reveals a close similarity of the relaxation functions  $\Gamma(\omega)$  to the behavior of the optical conductivity  $\sigma(\omega)$  which is the  $q \rightarrow 0$  property. The observed low- $\omega$  behavior  $\Gamma \sim \Gamma_0 + g\omega^\alpha$  indicates that the MBL transition is best characterized by the critical exponent  $\alpha = 1$ , consistent with several other numerical and renormalization-group analysis of dynamical quantities.<sup>21,22,24,25,54</sup> The extremely slow relaxation together



with finite time-windows, both in experiments as well in numerical studies, suggest that identifying MBL from the stiffness (i.e. from the saturated correlation functions) might be very challenging. Hence a more proper definition of the MBL should be related just to the critical dynamics, since this dynamics can be established within much shorter time-windows.

There are nevertheless clear open questions, e.g., whether  $\Gamma_0 > 0$  for arbitrary  $W < W_c$  (as well a d.c.  $\sigma_0 > 0$ )<sup>20,24,25</sup> or there exists intermediate regime with subdiffusive behavior<sup>21,22,63</sup> consistent with  $\Gamma_0 = 0$ . Beyond the fundamental importance, even more relevant is the question, whether experimental results on the imbalance relaxation could also confirm logarithmic character of relaxation towards the limiting nonergodic stiffnesses.<sup>37,51</sup>

### ACKNOWLEDGMENTS

M.M. acknowledges support from the 2015/19/B/ST2/02856 project of the Polish National Science Center. J.H. acknowledges the European Union program FP7-REGPOT-2012-2013-1 under grant agreement n. 316165. P.P. acknowledges the support by the program P1-0044 of the Slovenian Research Agency and of the Alexander von Humboldt Foundation, which allowed for the stay at the A. Sommerfeld Center for the Theoretical Physics, LMU München, and the Max-Planck Institute for Complex Systems, Dresden, where this work has been started.

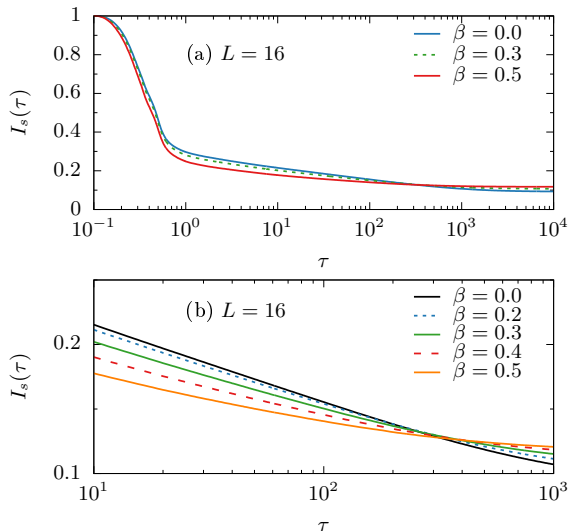


Figure 6. (Color online) Integrated correlation function  $I_s(\tau)$  obtained from exact diagonalization for  $L = 16$  and  $W = 4$  for various inverse temperatures  $\beta$ . Panel (b) shows the same as (a) but for the time-window  $10 < t < 1000$ .

### Appendix A: Results at finite temperatures

All the correlation functions discussed in the main text have been obtained at infinite temperature. While our numerical methods are inappropriate for the studies of the low-temperature regime, these methods provide reliable results also for large but finite temperatures. Here, we demonstrate that our main conclusion concerning the dynamics of correlation functions remain valid also in the latter regime, i.e., for the state  $\rho = \exp(-\beta H)/Z$ ,  $Z = \text{Tr}[\exp(-\beta H)]$  with the inverse temperature  $\beta \ll 1$ . Deep in the MBL regime one may formally assume the system to be in a thermal state. However such assumption may be unphysical simply because systems do not thermalize in the latter regime. In order to avoid this possible inconsistency we restrict our studies to the case  $W = 4$ , i.e., we stay close to the MBL transition.

At finite temperature, the real-time correlation function becomes

$$C_s(t) = \left\langle \frac{\text{Tr}(\rho O_s e^{iHt} O_s e^{-iHt})}{\text{Tr}(\rho O_s^2)} \right\rangle, \quad (\text{A1})$$

while the integrated spectra can be calculated from

$$I_s(\tau) = \int_{-1/\tau}^{1/\tau} d\omega C_s(\omega) = \left\langle \frac{\mathcal{I}_s(\tau)}{\mathcal{I}_s(\tau \rightarrow 0^+)} \right\rangle, \quad (\text{A2})$$

$$\mathcal{I}(\tau) = \sum_{\alpha, \alpha'} e^{-\beta E_\alpha} \theta \left( \frac{1}{\tau} - |E_\alpha - E_{\alpha'}| \right) |\langle \alpha | O_s | \alpha' \rangle|^2. \quad (\text{A3})$$

In Fig. 6 we show integrated correlation function,  $I_s(\tau)$ , obtained from the exact diagonalization for  $L = 16$ . The increase of  $\beta$  from 0 to 0.5 only weakly affects  $I_s(\tau)$ , as shown in figure 6a. As expected, the stiffness  $C(\infty) = I(\tau \rightarrow \infty)$  slightly increases with  $\beta$ . Unfortunately, the limited accuracy of the finite-size scaling of the disorder-averaged data does not allow us to judge whether the critical disorder for the MBL transition depends on  $\beta$ . However, results in Fig. 6 clearly show that our main claim concerning the extremely slow quasi-logarithmic decay of correlation functions remains valid also for large but finite temperatures.

### Appendix B: The reduced basis approach

Since we are interested in the MBL physics emerging from the non-interacting localized Anderson states  $|l\rangle$ , we introduce for comparison as well as for the closer insight the reduced basis approach (RBA). Taking  $\{|l\rangle\}$  as the basis of the single-particle space, we get

$$H_0 = H - H_V = \sum_l \epsilon_l \varphi_l^\dagger \varphi_l, \quad (\text{B1})$$

where  $\varphi_l^\dagger = \sum_i \langle i | l \rangle c_i^\dagger$  with  $H$  and  $H_V$  defined by Eqs. (1) and (2) in the main text. The interaction term,  $H_V$ , can be

then written in terms of localized states as

$$H_V = \sum_{k,l,m,n} V_{klmn} \varphi_k^\dagger \varphi_l^\dagger \varphi_m \varphi_n. \quad (\text{B2})$$

Considering the many-particle states within such localized basis

$$|\underline{m}\rangle = \prod_m \varphi_m^\dagger |0\rangle, \quad (\text{B3})$$

one should separately study the diagonal part of  $H_V$  denoted as the Hartree-Fock term,  $H_{HF}$ ,

$$\langle \underline{m} | H_{HF} | \underline{n} \rangle \propto \delta_{\underline{m}, \underline{n}}. \quad (\text{B4})$$

While  $|\underline{m}\rangle$  are eigenfunction of  $H_0 + H_{HF}$  with eigenvalues  $E_{\underline{m}}$ , the remaining  $H' = H_V - H_{HF}$  can induce the transitions between different  $\underline{m}$ . The RBA emerges from the consideration of systems with larger disorder  $W$ , where  $H'$  is the weakest term. Starting the dynamics from a chosen  $|\underline{m}\rangle$ , one can restrict the basis only to the states within the window  $|E_{\underline{n}} - E_{\underline{m}}| < \xi V$  with  $\xi \sim \mathcal{O}(1)$ . The goal is to use RBA with  $N_r \ll 2^L$  basis states and evaluate within it the dynamical quantity via a direct time evolution. In this way one may bypass and even monitor the question of MB resonances, the well known problem within the theory of localization<sup>1,5,54,64,65</sup>. We typically take  $N_r \simeq 4 \cdot 10^4$ .

In Fig. 7 we compare results for the integrated correlation functions obtained from various methods, see equations (8) and (9) in the main text. For  $\tau \leq 10^2$  results obtained from

exact diagonalization ( $L \leq 16$ ) nicely overlap with the data from RBA for  $L=20$ . While, the ED results saturate for larger  $\tau$ , the logarithmic decay continues apparently even further for  $L = 20$  up to the largest  $\tau \sim 2000$  available for the RBA. The comparison of results for different  $L$  confirms that the range of logarithmic decay can extend at least for one decade when increasing the system from  $L = 10$  to  $L = 20$ . It confirms also our main result that a more proper/practical definition of the MBL should be related to the critical dynamics rather than to stiffness. The latter quantity becomes available first after correlation functions saturate, while former one can be measured already during the relaxation.

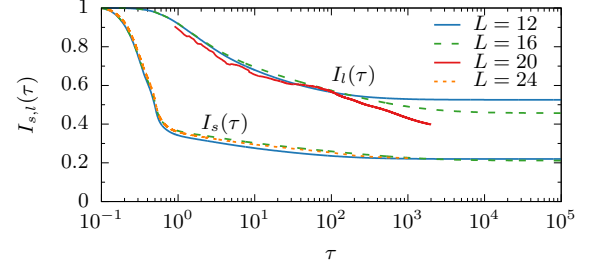


Figure 7. (Color online) Integrated correlation functions  $I_s(\tau)$  and  $I_l(\tau)$  obtained from exact diagonalization ( $L \leq 16$ ), reduced basis approach ( $L = 20$ ) and microcanonical Lanczos method ( $L = 24$ ) for disorder  $W = 5$ .

- <sup>1</sup> P. W. Anderson, “Absence of diffusion in certain random lattices,” *Phys. Rev.* **109**, 1492 (1958).
- <sup>2</sup> N. F. Mott, “Conduction in non-crystalline systems,” *Phil. Mag.* **17**, 1259 (1968).
- <sup>3</sup> B. Kramer and A. MacKinnon, “Localization: theory and experiment,” *Rep. Prog. Phys.* **56**, 1469 (1993).
- <sup>4</sup> F. Evers and A. D. Mirlin, “Anderson transitions,” *Rev. Mod. Phys.* **80**, 1355 (2008).
- <sup>5</sup> L. Fleishman and P. W. Anderson, “Interactions and the anderson transition,” *Phys. Rev. B* **21**, 2366 (1980).
- <sup>6</sup> D. M. Basko, I. L. Aleiner, and B. L. Altshuler, “Metal-insulator transition in a weakly interacting many-electron system with localized single-particle states,” *Ann. Phys.* **321**, 1126 (2006).
- <sup>7</sup> R. Modak and S. Mukerjee, “Many-body localization in the presence of a single-particle mobility edge,” *Phys. Rev. Lett.* **115**, 230401 (2015).
- <sup>8</sup> C. Monthus and T. Garel, “Many-body localization transition in a lattice model of interacting fermions: Statistics of renormalized hoppings in configuration space,” *Phys. Rev. B* **81**, 134202 (2010).
- <sup>9</sup> D. J. Luitz, N. Laflorencie, and F. Alet, “Many-body localization edge in the random-field heisenberg chain,” *Phys. Rev. B* **91**, 081103 (2015).
- <sup>10</sup> F. Andraschko, T. Enss, and J. Sirker, “Purification and many-body localization in cold atomic gases,” *Phys. Rev. Lett.* **113**, 217201 (2014).
- <sup>11</sup> C. R. Laumann, A. Pal, and A. Scardicchio, “Many-

- body mobility edge in a mean-field quantum spin glass,” *Phys. Rev. Lett.* **113**, 200405 (2014).
- <sup>12</sup> D. A. Huse, R. Nandkishore, and V. Oganesyan, “Phenomenology of fully many-body-localized systems,” *Phys. Rev. B* **90**, 174202 (2014).
- <sup>13</sup> P. Ponte, Z. Papić, F. Huveneers, and D. A. Abanin, “Many-body localization in periodically driven systems,” *Phys. Rev. Lett.* **114**, 140401 (2015).
- <sup>14</sup> A. Lazarides, A. Das, and R. Moessner, “Fate of many-body localization under periodic driving,” *Phys. Rev. Lett.* **115**, 030402 (2015).
- <sup>15</sup> R. Vasseur, S. A. Parameswaran, and J. E. Moore, “Quantum revivals and many-body localization,” *Phys. Rev. B* **91**, 140202 (2015).
- <sup>16</sup> M. Serbyn, Z. Papić, and D. A. Abanin, “Quantum quenches in the many-body localized phase,” *Phys. Rev. B* **90**, 174302 (2014).
- <sup>17</sup> D. Pekker, G. Refael, E. Altman, E. Demler, and V. Oganesyan, “Hilbert-glass transition: New universality of temperature-tuned many-body dynamical quantum criticality,” *Phys. Rev. X* **4**, 011052 (2014).
- <sup>18</sup> V. Oganesyan and D. A. Huse, “Localization of interacting fermions at high temperature,” *Phys. Rev. B* **75**, 155111 (2007).
- <sup>19</sup> T. C. Berkelbach and D. R. Reichman, “Conductivity of disordered quantum lattice models at infinite temperature: Many-body localization,” *Phys. Rev. B* **81**, 224429 (2010).
- <sup>20</sup> O. S. Barišić and P. Prelovšek, “Conductivity in a disordered one-dimensional system of interacting fermions,”

- Phys. Rev. B **82**, 161106 (2010).
- 21 K. Agarwal, S. Gopalakrishnan, M. Knap, M. Müller, and E. Demler, “Anomalous diffusion and griffiths effects near the many-body localization transition,” *Phys. Rev. Lett.* **114**, 160401 (2015).
  - 22 S. Gopalakrishnan, M. Müller, V. Khemani, M. Knap, E. Demler, and D. A. Huse, “Low-frequency conductivity in many-body localized systems,” *Phys. Rev. B* **92**, 104202 (2015).
  - 23 Y. Bar Lev, G. Cohen, and D. R. Reichman, “Absence of diffusion in an interacting system of spinless fermions on a one-dimensional disordered lattice,” *Phys. Rev. Lett.* **114**, 100601 (2015).
  - 24 R. Steinigeweg, J. Herbrych, F. Pollmann, and W. Brenig, “Scaling of the optical conductivity in the transition from thermal to many-body localized phases,” *ArXiv e-prints* (2015), 1512.08519 [cond-mat.stat-mech].
  - 25 O. S. Barišić, J. Kokalj, I. Balog, and P. Prelovšek, “Dynamical conductivity and its fluctuations along the crossover to many-body localization,” *ArXiv e-prints* (2016), 1603.01526 [cond-mat.stat-mech].
  - 26 M. Kozarzewski, P. Prelovšek, and M. Mierzejewski, “Distinctive response of many-body localized systems to a strong electric field,” *Phys. Rev. B* **93**, 235151 (2016).
  - 27 M. Žnidarič, T. Prosen, and P. Prelovšek, “Many-body localization in the heisenberg  $xxz$  magnet in a random field,” *Phys. Rev. B* **77**, 064426 (2008).
  - 28 J. H. Bardarson, F. Pollmann, and J. E. Moore, “Unbounded growth of entanglement in models of many-body localization,” *Phys. Rev. Lett.* **109**, 017202 (2012).
  - 29 J. A. Kjäll, J. H. Bardarson, and F. Pollmann, “Many-body localization in a disordered quantum ising chain,” *Phys. Rev. Lett.* **113**, 107204 (2014).
  - 30 M. Serbyn, Z. Papić, and D. A. Abanin, “Criterion for many-body localization-delocalization phase transition,” *Phys. Rev. X* **5**, 041047 (2015).
  - 31 D. J. Luitz, N. Laflorencie, and F. Alet, “Extended slow dynamical regime prefiguring the many-body localization transition,” *Phys. Rev. B* **93**, 060201 (2015).
  - 32 M. Serbyn, Z. Papić, and D. A. Abanin, “Universal slow growth of entanglement in interacting strongly disordered systems,” *Phys. Rev. Lett.* **110**, 260601 (2013).
  - 33 S. Bera, H. Schomerus, F. Heidrich-Meisner, and J. H. Bardarson, “Many-body localization characterized from a one-particle perspective,” *Phys. Rev. Lett.* **115**, 046603 (2015).
  - 34 A. Pal and D. A. Huse, “Many-body localization phase transition,” *Phys. Rev. B* **82**, 174411 (2010).
  - 35 M. Serbyn, Z. Papić, and D. A. Abanin, “Local conservation laws and the structure of the many-body localized states,” *Phys. Rev. Lett.* **111**, 127201 (2013).
  - 36 Y. Bar Lev and D. R. Reichman, “Dynamics of many-body localization,” *Phys. Rev. B* **89**, 220201 (2014).
  - 37 M. Schreiber, S. S. Hodgman, P. Bordia, H. P. Lüschen, M. H. Fischer, R. Vosk, E. Altman, U. Schneider, and I. Bloch, “Observation of many-body localization of interacting fermions in a quasi-random optical lattice,” *Science* **349**, 842 (2015).
  - 38 V. Khemani, R. Nandkishore, and S. L. Sondhi, “Nonlocal adiabatic response of a localized system to local manipulations,” *Nat. Phys.* **11**, 560 (2015).
  - 39 I. V. Gornyi, A. D. Mirlin, and D. G. Polyakov, “Interacting electrons in disordered wires: Anderson localization and low- $t$  transport,” *Phys. Rev. Lett.* **95**, 206603 (2005).
  - 40 E. Altman and R. Vosk, “Universal dynamics and renormalization in many-body-localized systems,” *Annu. Rev. Condens. Matter Phys.* **6**, 383 (2015).
  - 41 A. De Luca and A. Scardicchio, “Ergodicity breaking in a model showing many-body localization,” *EPL (Europhysics Letters)* **101**, 37003 (2013).
  - 42 C. Gramsch and M. Rigol, “Quenches in a quasidisordered integrable lattice system: Dynamics and statistical description of observables after relaxation,” *Phys. Rev. A* **86**, 053615 (2012).
  - 43 A. De Luca, B. L. Altshuler, V. E. Kravtsov, and A. Scardicchio, “Anderson localization on the Bethe lattice: Nonergodicity of extended states,” *Phys. Rev. Lett.* **113**, 046806 (2014).
  - 44 D. A. Huse, R. Nandkishore, V. Oganesyan, A. Pal, and S. L. Sondhi, “Localization-protected quantum order,” *Phys. Rev. B* **88**, 014206 (2013).
  - 45 M. Serbyn, M. Knap, S. Gopalakrishnan, Z. Papić, N. Y. Yao, C. R. Laumann, D. A. Abanin, M. D. Lukin, and E. A. Demler, “Interferometric probes of many-body localization,” *Phys. Rev. Lett.* **113**, 147204 (2014).
  - 46 Rahul N. and D. A. Huse, “Many-body localization and thermalization in quantum statistical mechanics,” *Annu. Rev. Condens. Matter Phys.* **6**, 15 (2015).
  - 47 L. Rademaker and M. Ortuño, “Explicit local integrals of motion for the many-body localized state,” *Phys. Rev. Lett.* **116**, 010404 (2016).
  - 48 A. Chandran, I. H. Kim, G. Vidal, and D. A. Abanin, “Constructing local integrals of motion in the many-body localized phase,” *Phys. Rev. B* **91**, 085425 (2015).
  - 49 V. Ros, M. Müller, and A. Scardicchio, “Integrals of motion in the many-body localized phase,” *Nuclear Physics B* **891**, 420 (2015).
  - 50 S. S. Kondov, W. R. McGehee, W. Xu, and B. DeMarco, “Disorder-induced localization in a strongly correlated atomic hubbard gas,” *Phys. Rev. Lett.* **114**, 083002 (2015).
  - 51 P. Bordia, H. P. Lüschen, S. S. Hodgman, M. Schreiber, I. Bloch, and U. Schneider, “Coupling identical 1D many-body localized systems,” *Phys. Rev. Lett.* **116**, 140401 (2016).
  - 52 M. Boll, T. A. Hilker, G. Salomon, A. Omran, I. Bloch, and C. Gross, “Spin and charge resolved quantum gas microscopy of antiferromagnetic order in Hubbard chains,” *ArXiv e-prints* (2016), 1605.05661 [cond-mat.stat-mech].
  - 53 R. Vosk, D. A. Huse, and E. Altman, “Theory of the many-body localization transition in one-dimensional systems,” *Phys. Rev. X* **5**, 031032 (2015).
  - 54 A. C. Potter, R. Vasseur, and S. A. Parameswaran, “Universal properties of many-body delocalization transitions,” *Phys. Rev. X* **5**, 031033 (2015).
  - 55 M. W. Long, P. Prelovšek, S. El Shawish, J. Karadamoglou, and X. Zotos, “Finite-temperature dynamical correlations using the microcanonical ensemble and the lanczos algorithm,” *Phys. Rev. B* **68**, 235106 (2003).
  - 56 P. Prelovšek and J. Bonča, “Ground state and finite temperature lanczos methods,” in *Strongly Correlated Systems - Numerical Methods*, edited by A. Avella and F. Mancini (Springer, Berlin, 2013).
  - 57 P. Sierant, D. Delande, and J. Zakrzewski, “Many-body localization due to random interactions,” *ArXiv e-prints* (2016), 1607.00227 [cond-mat.stat-mech].
  - 58 Sarang Gopalakrishnan, Kartiek Agarwal, Eugene A. Demler, David A. Huse, and Michael Knap, “Griffiths effects and slow dynamics in nearly many-body localized systems,” *Phys. Rev. B* **93**, 134206 (2016).
  - 59 Kartiek Agarwal, Eugene Demler, and Ivar Martin, “ $1/f^\alpha$  noise and generalized diffusion in random heisenberg spin systems,” *Phys. Rev. B* **92**, 184203 (2015).
  - 60 H. Mori, “Transport, collective motion, and brownian motion,” *Prog. Theor. Phys.* **33**, 423 (1965).
  - 61 W. Götze and P. Wölfle, “Homogeneous dynamical conductivity of simple metals,” *Phys. Rev. B* **6**, 1226 (1972).

- <sup>62</sup> D. Forster, *Hydrodynamic Fluctuations, Broken Symmetry, And Correlation Functions* (Westview Press, New York, 1995).
- <sup>63</sup> M. Žnidarič, M. Scardicchio, and V. K. Varma, “Diffusive and subdiffusive spin transport in the ergodic phase of a many-body localizable system,” [ArXiv e-prints \(2016\)](#), 1604.08567 [cond-mat.stat-mech].
- <sup>64</sup> R. Vosk and E. Altman, “Many-body localization in one dimension as a dynamical renormalization group fixed point,” [Phys. Rev. Lett. \*\*110\*\*, 067204 \(2013\)](#).
- <sup>65</sup> J. Z. Imbrie, “Diagonalization and many-body localization for a disordered quantum spin chain,” [ArXiv e-prints \(2016\)](#), 1605.03003 [cond-mat.stat-mech].